Foundational Fuel Chemistry Model 2 — Can data assimilation yield useful insights in reaction rate constants?

Yue Zhang[a], Wendi Dong[a], Andrea Nobilli[a], Ryan F. Johnson[b], Gregory P. Smith[c], Hai Wang[a,]

[a]*Department of Mechanical Engineering, Stanford University, Stanford, CA 94305, United States*
[b]*Laboratories for Computational Physics and Fluid Dynamics, U.S. Naval Research Laboratory, 4555 Overlook Ave SW, Washington, DC 20375, United States*
[c]*SRI International, Menlo Park, CA 94025, United States*

Abstract

The foundation fuel chemistry model version 2 (FFCM-2), consisting of 96 species and 1054 reactions, is a recently developed reaction model for $C_{0\text{-}4}$ hydrocarbon combustion. In the development of FFCM-2, reaction rate constants, primarily sourced from reaction rate theory and experiments, were evaluated for their uncertainties. Optimization and uncertainty minimization were conducted using a neural-network based method of uncertainty minimization employing polynomial chaos expansions (NN-MUM-PCE), which assimilated over 1,000 sets of legacy combustion property data while ensuring that all rate constants adhered to their associated physical constraints and uncertainty bounds. The current study focuses on an analysis of the optimized and uncertainty minimized reaction rate constants. By comparing the trial and optimized rate constants with literature data, we demonstrate that large-scale data assimilation, when combined with appropriate physical constraints, can effectively minimize rate uncertainties, identify missing reactions and improvements to the reaction pathways, and provide valuable insights into individual rate constants.

Keywords: Data Assimilation, Foundational Fuel Chemistry Model, Uncertainty Quantification

Novelty and significance statement

A detailed combustion reaction model, FFCM-2, has been developed by assimilating a comprehensive combustion experiment database for $C_{0\text{–}4}$ fuels. It is a common challenge to assure a necessary completeness of the reaction set in a kinetic model. The data assimilation approach used in FFCM-2 development can identify if there is missing reaction. Despite of abundant studies on various reaction rates, many of them still remain large uncertainties in literature. The data assimilation approach can constrain their uncertainties.

1. Introduction

Predictive combustion kinetic models play an essential role in combustor design and optimization. A kinetic model for heavier hydrocarbon fuels relies on a foundational fuel chemistry model that accurately describes the reaction chemistry of H_2, CO, and $C_{1\text{-}4}$ hydrocarbons. Foundational fuel chemistry models consist of thousands of elementary reactions, each of which has a rate constant and an associated uncertainty. As a multi-parameter problem, such a large parameter set makes it challenging to arrive at a predictive model [1, 2]. Thus, understanding reaction pathways at the fundamental level and quantitatively determining individual rate constants are central to the development of predictive kinetic models.

Progress has been made in producing accurate individual reaction rate constants over the past few decades. Decades of experimental measurements of combustion fundamental properties including laminar flame speeds, ignition delay time, and species time-histories obtained from experiments provided valuable insights into fundamental understanding of reaction pathways and their associated rate constants. The recent advancement of laser diagnostics and shock tube experiments enables direct measurements of certain reaction rates, such as $H + O_2 \rightleftharpoons OH + O$, with uncertainties less than 10% [2, 3]. In addition, the application of quantum chemistry calculations and reaction rate theory have advanced to a level that produces accurate rate parameters for reactions that can be used for predicting rates beyond existing experimental conditions [4].

Data assimilation plays an essential role in model development [5, 2], by combining the state of knowl-

edge on reaction rate parameters and combustion fundamental property data using globally constrained, systematic optimization. Past efforts include the GRI Mech [6] for CH_4 combustion, an optimized C_3H_8 reaction model by Qin et al. [7] and a H_2-CO reaction model by Davis et al. [8] using the solution mapping approach [5]. Notably, the foundational fuel chemistry model version 1.0 (FFCM-1), developed for [9] for H_2, CO and CH_4 combustion, employed the method of uncertainty minimization using polynomial chaos expansions (MUM-PCE) approach for both optimization and uncertainty minimization (UM). Other recent, related efforts include reaction models developed for combustion of H_2 [10], H_2/syngas [11], ethanol [12], ethane [13], formaldehyde and methanol [14, 15].

Recently, we proposed the foundational fuel chemistry model version 2 (FFCM-2) [16], which consists of 96 species and 1,054 reactions, covering the combustion chemistry of H_2, H_2O_2, CO, and 19 $C_{1-4}H_xO_y$ fuels. The narrowed rate uncertainty and improved predictive accuracy of FFCM-2 were the results of the method of uncertainty minimization using polynomial chaos expansions (MUM-PCE) [17, 18] which leveraged a neural network based approach, NN-MUM-PCE [19]. The resulting reaction model assimilated 1,192 legacy combustion property targets during optimization as detailed in [16, 20, 21].

In our previous work [21], we demonstrated that large-scale data assimilation in FFCM-2 could identify missing reactions. The work presented here further aims to evaluate whether data assimilation and systematic optimization can yield useful kinetic insights and reduce uncertainties in rate constants.

2. Methods

This section provides an overview of the process for developing a chemical reaction model using data assimilation to minimize model prediction uncertainty. For a more in-depth mathematical description, we refer the reader to [16, 20, 21].

2.1. Data assimilation for chemical reaction model development with uncertainty minimization

Mathematically, the canonical MUM-PCE solves a constrained optimization problem to obtain rate parameters which minimize the objective function,

$$\min_{\boldsymbol{x}} \Phi(\boldsymbol{x}) = \min_{\boldsymbol{x}} \left\{ \sum_{m=1}^{M} \left(\frac{y_m(\boldsymbol{x}) - y_{m,\mathrm{exp}}}{\sigma_{m,\mathrm{exp}}} \right)^2 + \|\lambda \boldsymbol{x}\|_2^2 \right\}, \quad s.t., \boldsymbol{x} \in [\boldsymbol{-1}, \boldsymbol{1}]. \tag{1}$$

Here $\boldsymbol{x}$ is a vector of perturbed reaction rate constants for the n_r reactions that can be analyzed, $\boldsymbol{x} = (x_1, \ldots, x_{n_r})$. The perturbed reaction rates are normalized using the expression $x_k = \ln(A_k/A_{k,0})/\ln f_k$ where the index k refers to the reaction of interest, A_k is the pre-exponential factor of the k^{th} reaction rate, $A_{k,0}$ is the nominal, unperturbed, pre-exponential factor, and f_k is the uncertainty factor for the reaction rate. In Eq. (1), the perturbed reaction rate constants are used in a predictive model to yield a target system response quantity, such as flame speed or induction time. In Eq. (1), the target $y_m(\boldsymbol{x})$ is a model prediction of the target quantity, $y_{m,\mathrm{exp}}$ is the observed experimental quantity, and $\sigma_{m,\mathrm{exp}}$ is the uncertainty of the experimental quantity. Here, the subscript m is for the m^{th} target quantity for a total of M quantities. Finally, λ is a regularization coefficient that governs the weighting factor between the rate parameters, $\boldsymbol{x}$, and the mean square error of the model prediction. Without the presence of the $\|\lambda \boldsymbol{x}\|_2^2$ term, i.e., $\lambda \to 0$, the objective function would lack any bias associated with the nominal rate constants, effectively reducing their influence on the optimization process. In this work, $\lambda = 4$ was chosen to balance the weighting between the reaction kinetics and legacy combustion target quantities [22].

The MUM-PCE approach targets the minimization of reaction rate uncertainties which inherently minimizes Φ. This is achieved using a gradient descent method, which iteratively minimizes uncertainty by starting from a trial model and progressively updating it to find an optimized model. The gradient descent method requires the Jacobian of the objective function with respect to reaction rate parameters, $\partial\Phi/\partial\boldsymbol{x}$. By examining Eq. (1), $\partial\Phi/\partial\boldsymbol{x}$ depends on $\boldsymbol{x}$, $\boldsymbol{y}(\boldsymbol{x})$, and the Jacobian of the target function, $\mathbf{J} = \partial\boldsymbol{y}(\boldsymbol{x})/\partial\boldsymbol{x}$. In the development of FFCM-2, we utilized a fully connected deep neural network to produce an estimate of $\boldsymbol{y}(\boldsymbol{x})$ and thus the Jacobian is immediately available due to the automatic differentiability of the neural network. This is the NN component of NN-MUM-PCE.

2.2. Freezing unconstrained parameters

NN-MUM-PCE is capable of perturbing and optimizing all reaction rates rather than pre-selecting a set of active parameters using a linear sensitivity analysis which was previously done for FFCM-1. However, experiments are not sensitive to all reactions, and therefore only a subset of rate parameters should be constrained by experimental data. In this work, an unconstrained parameter x_k is declared to not contribute to improving model prediction or reducing the prediction uncertainty if $|A_k/A_{k,0} - 1| < \chi_A$ and the optimized uncertainty of x_k is larger than χ_σ, where χ_A is the multiplier threshold and χ_σ is the uncertainty threshold. To suppress noise, we apply a conditional normal distribution to fix the effect of the unconstrained parameters on the distribution of the normalized rate coefficients, $\boldsymbol{x}$, as outlined in [19]. In addition, we performed a parametric study that led to $\chi_A = 0.05$ and $\chi_\sigma = 0.48$, which gave 258 active rate parameters [19].

3. Results and Discussion

In this section, we provide an overall analysis of the perturbed rate parameters after data assimilation. We then report several case studies from the FFCM-2 effort to demonstrate that properly constrained optimization and data assimilation provide useful kinetic insights, e.g., discover missing reactions and refine the newly proposed rate constants, identify limitations in branching ratios, minimize uncertainties of existing reactions and unveil kinetic coupling between key reaction pathways.

3.1. Overall rate parameter perturbations after data assimilation

Among the 258 rate parameters constrained in FFCM-2, only ten see changes of $|x_k| > 0.4$. Figure 1 lists the top ten most perturbed rate parameters, ranked by the absolute values of x_k in a descending order. In this figure the trial parameter rate data and their distributions are shown as a blue line for each reaction, centered around the normalized trial mean. The red dot represents the nominal optimized rate parameter, with a corresponding red line representing its uncertainty. This figure shows that the nominal trial and nominal optimized rates are indeed different and that the NN-MUM-PCE method has minimized the resulting uncertainties. By investigating the factors that influence the changes between these trial and optimized rates and comparing with literature, valuable insights to improve rate coefficients can be gained. In what follows, we demonstrate this point with selected rate parameters from these top-ten reactions.

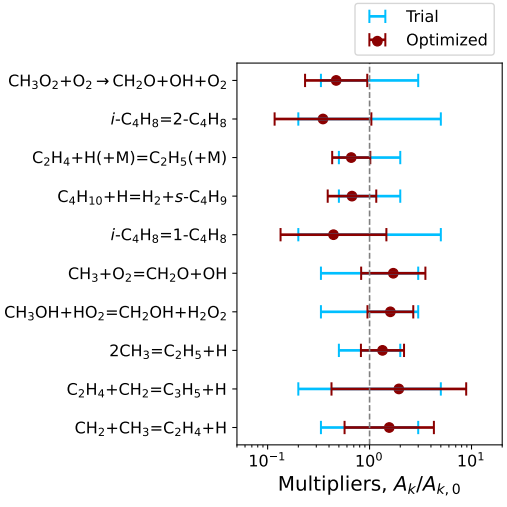

Fig. 1: Comparisons of the mean and 2σ (95% confidence interval) of the top 10 most perturbed rate parameters of FFCM-2 before (blue) and after (red) optimization and uncertainty minimization.

3.2. Including missing reactions and minimizing their rate uncertainties

Data assimilation offers insights into missing reaction pathways [20, 21]. In an earlier work [20], we discussed the refinements of iso-butene isomerization reactions (i-$C_4H_8 \rightleftharpoons$ 1-C_4H_8 and i-$C_4H_8 \rightleftharpoons$ 2-C_4H_8) in order to reproduce shock tube pyrolysis data. In a recent work, we also investigated the HCO prompt dissociation reactions and their impact on reconciling laminar flame speed of C_2H_2 and CH_2O [21]. In this work, we illustrate this point with another example: the reaction of CH_3O_2 + O_2 and its impact on high-pressure methane ignition.

An increased interest in high-pressure gas turbines burning natural gas makes it essential to have a reaction model that can reliably predict CH_4 combustion at high pressure and high O_2 concentrations. The initial version of the trial model drastically overpredicted methane ignition delay times at a high O_2 to diluent ratio and for pressures >150 atm, as shown in Fig. 2. The measured ignition delay times could not be attained by adjusting relevant rate parameters within their uncertainty bounds. This result points to the need of including missing reactions in the kinetic model. The observation inspired Lakshmanan et al. [23] to investigate the reactions of CH_3O_2 + O_2 using quantum chemistry calculations and classical trajectory calculations, which identified the following two key reaction channels, as listed in Reaction (2) and Reaction (3):

$$\begin{aligned} &\mathrm{CH_3O_2 + O_2 \rightarrow CH_2O + OH + O_2},\\ &k = 4.2\times10^{13}\exp(-8676/T)\ \mathrm{cm^3 mol^{-1} s^{-1}}; \end{aligned} \tag{2}$$

$$\begin{aligned} &\mathrm{CH_3O_2 + O_2 \rightarrow HO_2 + CO + H_2O},\\ &k = 467T^{2.9}\exp(-20870/T)\ \mathrm{cm^3 mol^{-1} s^{-1}}. \end{aligned} \tag{3}$$

Reaction (2) consumes CH_3O_2 to produce OH radical, that boosts the reactivity. Figure 3 shows that prohibiting CH_3 recombination would significantly slow down the reactivity without Reaction (2). However, by applying these trial rate constants from [23] lead to improvement in accuracy with slight underprediction. In FFCM-2, NN-MUM-PCE generated the optimized rate constant of Reaction (2) which reduced to 47% of its trial value ($x = -0.687$, the largest deviation from trial rates in FFCM-2 optimization). In addition, the uncertainty factor reduced from $f_{\mathrm{trial}} = 3.0$ to $f_{\mathrm{opt}} = 2.0$. With this optimization, FFCM-2 predicts high-pressure methane and natural gas ignition with improved accuracy. In the optimization process, the minor pathway Reaction (3) was determined as an unconstrained parameter with its trial rate constant unchanged, indicating the efficacy of our approach in suppressing noise in the assimilation of the FFCM-2 dataset. Figure 3 reports the most sensitive reactions for predicting high-pressure methane ig-

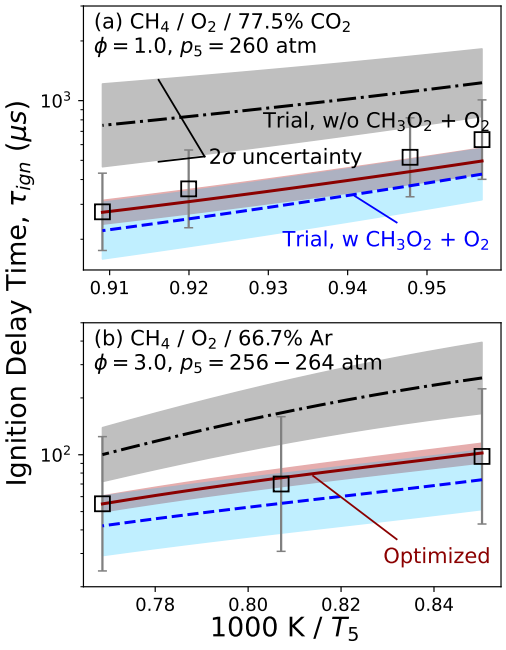

Fig. 2: Experiments and model predictions of CH_4 ignition delay under high-pressure and high-O_2 concentration condition. Experimental data are from (a) Shao et al. [24], (b & c) Petersen et al. [25]. Solid and dashed lines are optimized and trial model predictions, respectively.

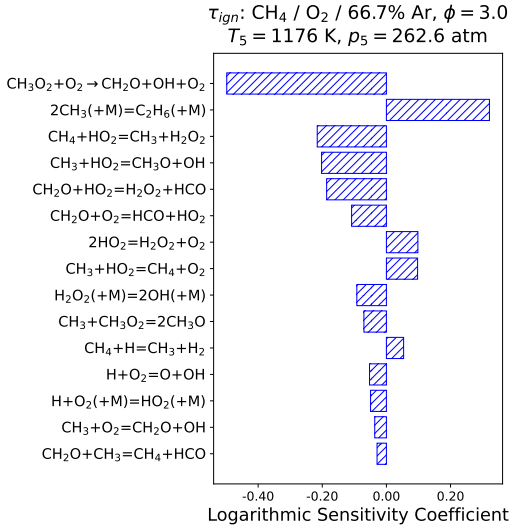

Fig. 3: Ranked sensitivity coefficient for ignition delay time of CH_4 / O_2 mixture in 667.7% argon with equivalence ratio $\phi = 3.0$, $T_5 = 1176$ K and $p_5 = 262.6$ atm. The thermodynamic condition studied is taken from Petersen et al [25], which is plotted in Fig. 2b.

nition delay time using the optimized rates of FFCM-2. Here, Reaction (2) exhibits the highest sensitivity which justifies its inclusion and uncertainty minimization.

3.3. Branching ratio and reactions for high temperature ethylene ignition

Another observation from the initial version of the trial model is the over-prediction of C_2H_4 ignition delay times under high O_2 concentrations, especially at elevated temperatures. The disagreement is attributed to the branching ratio of the C_2H_4 + O reactions. We adjusted the rates to match the branching ratio, ensuring agreement with experimental ignition delay times. These changes were added into the trial model and were optimized over the entire data base of available experimental data using NN-MUM-PCE.

The initial trial model used the branching ratio reported by Baulch et al. [26] based on a series of low-temperature experiments, where they recommended the product branching ratio to be 60% CH_3 + HCO, 35% CH_2CHO + H, and 5% CH_2CO + H_2. Recently, Li et al. [27] investigated the C_2H_4 + O system using an ab initio theory and master equation modeling approach. Figure 4 compares the branching ratio of the two studies for temperatures ranging from 250 K to 1750 K. It is observed that Li's new calculations are consistent with those of Baulch et al. [26] at low temperature., however at high temperature the recent theory predicts CH_2CHO + H and CH_2 + CH_2O to be the major products rather than CH_3 + HCO.

Figure 5 shows that with the branching ratio recommended by Baulch et al. [26] that the ignition delay time for C_2H_4 / air mixture (panel (a)) and C_2H_4/O_2 in 84% Ar (panel (c)) is over-predicted and outside of the 2σ data uncertainty due to the domination of inhibiting CH_3 + HCO pathway. The branching ratio of Li et al. accelerates the kinetics as CH_2CHO + H promotes the reactivity, and the improved trial model predicts experiments within their respective uncertainties. The observation here again demonstrates that reaction rate theories are critical to rate evaluation. If the branching ratio calculated by Li et al. [27] is applied as is, only minor under-prediction was observed for the C_2H_4 / air mixtures, as shown in Fig. 5a.

Figure 6 shows the result of a sensitivity analysis for the C_2H_4 / air mixture plotted in Fig. 5a. The rate limiting reaction is the same, before and after the C_2H_4 + O branching ratio update, as the system is dominated by the chain branching reaction H + O_2 $\rightleftharpoons$ O + OH. With the branching ratio of Baulch et al. [26], the inhibiting CH_3 + HCO channel has a larger sensitivity than the promoting channel CH_2CHO + H. The branching ratio by Li et al. [27] reduces the importance of the inhibiting CH_3 + HCO channel. The pathway of CH_2CHO + H is favored, and the H atom production promotes the reactivity.

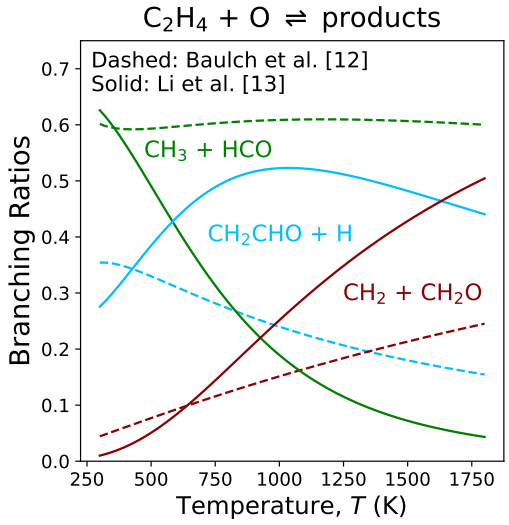

Fig. 4: Branching ratio of the C_2H_4 + O system for products CH_3 + HCO (green), CH_2CHO + H (blue) and CH_2 + CH_2O (red) as a function of temperature T. The dashed lines represent the recommendation from Baulch et al. [26] and the solid lines represent the calculation by Li et al. [27]. For Baulch et al.'s recommendation, all three pathways are shown. For Li et al.'s calculation, only the three major pathways (branching ratio larger than 5%) are illustrated.

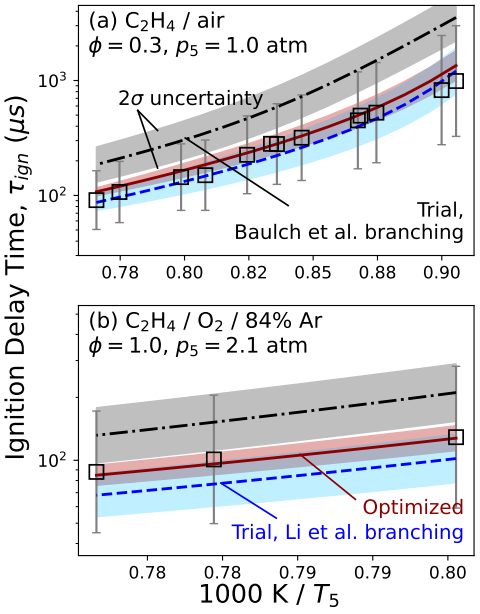

Fig. 5: C_2H_4 ignition delay times predicted by trial FFCM-2 (blue dashed lines) with C_2H_4 + O branching from Li et al. [27], optimized FFCM-2 (red solid lines), and trial FFCM-2 with C_2H_4 + O branching from Baulch et al. [26] under various thermodynamic conditions. Panel (a): C_2H_4 / air, ϕ = 0.3, p_5 = 1.0 atm, experimental data from Gillespie [28]; panel (b): C_2H_4-O_2 in 84% Ar as bath gas, ϕ = 1.0, p_5 = 2.1 atm, experimental data from Horning [29]. The gray vertical bars represent 2σ data uncertainties. The shaded areas represent 2σ model prediction uncertainties.

3.4. Minimizing uncertainties of existing reaction rate parameters

Despite extensive efforts to develop accurate reaction rate parameters, several reactions in existing kinetic models still exhibit large uncertainties. In this section, we demonstrate that data assimilation is an effective tool to improve individual rate constants by leveraging information from both reaction rate theory and target combustion properties. We demonstrate this with trial and optimized rate constants for three selected rate constants and compare them with the data in literature.

3.4.1. $CH_3 + O_2 \rightleftharpoons CH_2O + OH$

The reaction of methyl radical with molecular oxygen,

$$CH_3 + O_2 \rightleftharpoons CH_2O + OH, \qquad (4)$$

has notable impact to ignition delay of methane, alkanes, and several oxygenated fuels like acetone (CH_3COCH_3). Even with extensive focus in previous work [30, 31, 32, 33, 34, 35], the uncertainty of Reaction (4) remains large. For example, at temperature T = 1000 K, the literature data differs by approximately a factor of 20 between the extrapolated rate expression from the shock tube measurements by Srinivisan et al. [32] and GRI-Mech 1.3 [30].

In FFCM-2, the rate coefficient from Herbon et al. [33] was adopted in the trial model, which was derived by examining the kinetics of CH_3 + O_2 in high-temperature shock tube experiments over the temperature range 1590–2430 K. The optimized rate constant increased the trial values by a factor of 1.71 (x = 0.48) and reduced the uncertainty from f_{trial} = 3.0 to f_{opt} = 2.1. As shown in Fig. 7a, the optimized rate from data assimilation aligns closely with Klippenstein's theoretical study (incorporated into the 2013 Aramco model [34]), demonstrating confidence in the accuracy of our approach.

The rate constants for Reaction (4) at temperatures above 1500 K are fairly consistent with all literature data falling within a factor of 3. For the temperature range of 1000 K to 1500 K, the uncertainty in experimental analyses are notably larger than those from reaction rate theories. This could be attributed to the uncertainty in the extrapolation of high temperature measurements to lower temperature regions. In addition, determining the rate constant of Reaction (4) within the temperature range 1000 K to 1500 K, could be difficult due to the strong cou-

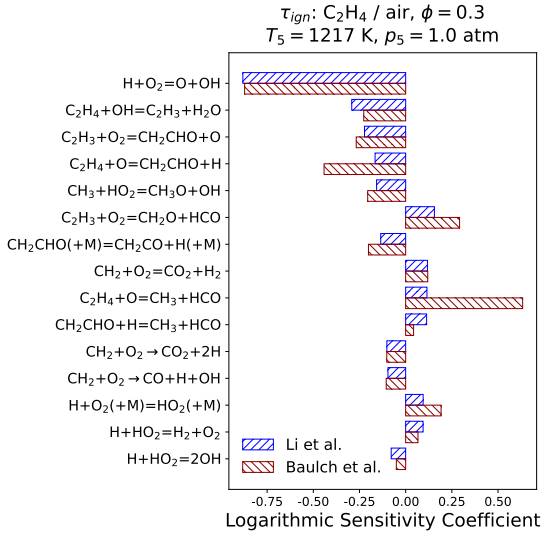

Fig. 6: Ranked sensitivity coefficient for ignition delay time of C_2H_4 / air mixture with equivalence ratio $\phi = 0.3$, $T_5 = 1217$ K and $p_5 = 1.0$ atm. The thermodynamic condition studied is taken from Gillipse [28], which is plotted in Fig. 5a.

pling with several other reaction pathways, notably $CH_3 + O_2 \rightleftharpoons CH_3O + O$, $CH_3 + HO_2 \rightleftharpoons CH_3O + OH$ and $CH_3 + HO_2 \rightleftharpoons CH_4 + O_2$, which will be further discussed in Section 3.5. The optimization analysis presents unique advantages in improving the individual rate constant in Reaction (4) as it factors in the kinetic coupling of other reactions and systematic data constraints from a diverse set of targets beyond methane ignition.

3.4.2. $CH_3OH + HO_2 \rightleftharpoons CH_2OH + H_2O_2$

The trial rates of the reaction,

$$CH_3OH + HO_2 \rightleftharpoons CH_2OH + H_2O_2, \qquad (5)$$

sourced from reaction rate theory calculations by Alecu and Truhlar [36], caused over-prediction of CH_3OH ignition delays. In FFCM-2, the resulting optimized rate constants were a factor of 1.60 of its trial value ($x = 0.427$), while the uncertainty factor was reduced from $f_{\text{trial}} = 3$ to $f_{\text{opt}} = 1.67$.

Figure 7b presents several recently reported rate constants for Reaction (5). Three theoretical analyses were conducted in 2011 by Klippenstein et al. [37], Altarawneh et al. [38], and Alecu and Truhlar [36]. At a temperature of $T = 1000$ K, the rate coefficient from Altarawneh et al. [38] is 16 times higher than that of Klippenstein et al. [37], while the rate constant from Alecu and Truhlar [36] falls between the two, being three times higher than Klippenstein et al. [37]. More recently, Olm et al. [14] performed a reaction model optimization for methanol and formaldehyde combustion. The FFCM-2 optimized rate constant aligns with the values reported by Olm et al. [14] and Altarawneh et al. [38] at high temperatures, although some discrepancies are observed at temperatures of 1000 K and below.

3.4.3. $n\text{-}C_4H_{10} + H \rightleftharpoons p\text{-}C_4H_9 + H_2$ and $n\text{-}C_4H_{10} + H \rightleftharpoons s\text{-}C_4H_9 + H_2$

H-abstraction reactions are key reactions initiating the breakdown of long-chain alkanes (e.g., reactions (6), (7) for normal butane). H-abstraction reactions creates the intermediates p-C_4H_9 and s-C_4H_9 which subsequently undergo β-scission to produce C_2H_4 and C_2H_5 or C_3H_6 and CH_3 at elevated temperature. The trial rates that dictate the production of these intermediates via the reactions,

$$n\text{-}C_4H_{10} + H \rightleftharpoons p\text{-}C_4H_9 + H_2, \qquad (6)$$
$$n\text{-}C_4H_{10} + H \rightleftharpoons s\text{-}C_4H_9 + H_2, \qquad (7)$$

were derived by scaling the rate constants of primary and secondary abstraction reactions $C_3H_8 + H$ to match the experiments for n-C_4H_{10} at temperature $T = 753$ K from Baker et al. [43]. Despite its consistency with rate constants derived from a joint effort of shock tube measurements and ab initio transition state theory by Peukert et al. [42], the trial rates caused slight over-prediction of n-C_4H_{10} ignition delay. In FFCM-2, the optimized rates decreased the A-factor of Reaction (7) by 33% ($x = -0.57$), while reducing the uncertainty factor from $f_{\text{trial}} = 2.0$ to $f_{\text{opt}} = 1.73$. Figure 7c shows that the optimized rates align with the rate constant reported by Manion et al. [39], where they studied the rate constants using shock tube species measurements and the MUM-PCE framework. The optimized rate constant was also found to be consistent with the recommendation from Cohen [40] at high temperatures ($T > 1500$ K), despite a slight discrepancy at around 1000 K.

3.4.4. Ethyl radical decomposition

The trial rates of the reaction,

$$C_2H_4 + H\,(+M) \rightleftharpoons C_2H_5\,(+M), \qquad (8)$$

was sourced from the theoretical calculation by Miller and Klippenstein [44], which led to over-prediction of ethane flame speeds and under-prediction of ignition delay times, as shown in Figs. 8 and 9, respectively. The over-prediction of reactivity was attributed to the fact that Reaction (8) occurs in the reverse direction during ethane combustion, decomposing ethyl radicals into C_2H_4 and H. The resulting H radical leads to increased reactivity of the system.

Similar over-predictions of reactivity have been reported in other works. For example, USC Mech II has been shown to overestimate reactivity relative to experiments across a range of conditions

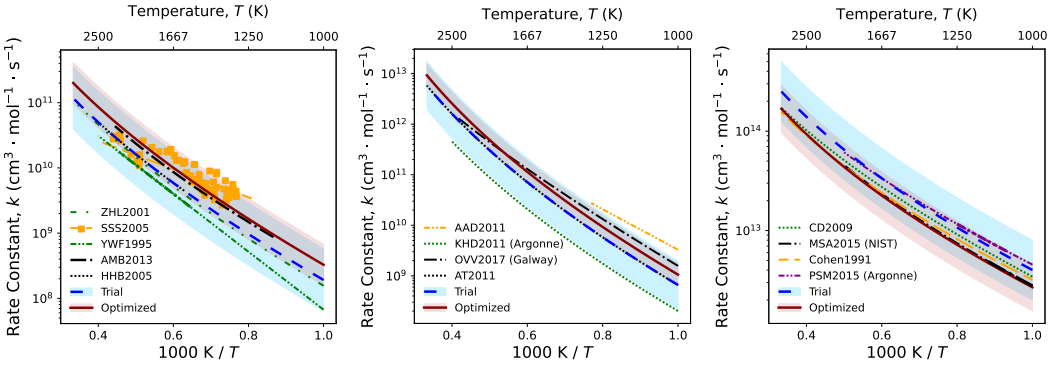

(a) $CH_3 + O_2 \rightleftharpoons CH_2O + OH$ (b) $CH_3OH + HO_2 \rightleftharpoons CH_2OH + H_2O_2$ (c) $n\text{-}C_4H_{10} + H \rightleftharpoons s\text{-}C_4H_9 + H_2$

Fig. 7: Comparison of rate coefficients in trial (dashed) and optimized (solid) FFCM-2 with literature data for three selected reactions, with the shaded areas indicating trial and optimized rate uncertainties. Left panel: Herbon et al. [33] (HHB2005), Srinivasan et al. [32] (SSS2005), Zhu et al. [31] (ZHL2001), Aul et al. [34] (AMB2013) and Yu et al. [30] (YWF1995); Middle panel: Alecu and Truhlar [36] (AT2011), Klippenstein et al. [37] (KHD2011), Altarawneh et al. [38] (AAD2011) and Olm et al. [14] (OVV2017); Right panel: Manion et al. [39] (MSA2015), Cohen [40] (Cohen 1991), Carstensen and Dean [41] (CD2009) and Peukert et al. [42] (PSM2015).

and mixtures[45, 46, 47, 48, 49]. Additionally, research done by [50] found better agreement to high-temperature ignition delays for C_2H_6 and CH_4/C_2H_6 by reducing the high-pressure and low-pressure limits of Reaction (8) by 30% for the Aramco Mech. In this work, the data assimilation resulted in reducing the high-pressure and low-pressure rate limits of the rate coefficients by 66% of their trial values ($x = -0.592$). Additionally, the uncertainty factor reduced from $f_{\text{trial}} = 2.0$ to $f_{\text{opt}} = 1.53$. The optimized rate parameter is consistent with the results of ad hoc tuning in various studies of ethane combustion, such as [45, 46, 47, 48, 49].

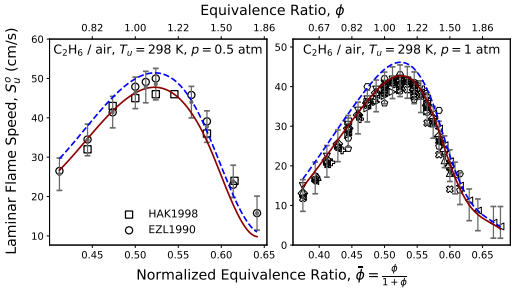

Fig. 8: Laminar flame speeds predicted by the trial (dashed lines) and optimized (solid lines) FFCM-2 for C_2H_6/air mixtures at unburned temperature $T_u = 298$ K, pressure $p = 0.5$ atm (left panel) and pressure $p = 1.0$ atm (right panel). Vertical error bars are data uncertainties. Symbols are experimental data. Left panel: Hassan et al. [51] (HAK1998), Egolfopoulos et al. [52] (EZL1990). Right panel: □ Goswami et al. [53], ○ Ravi et al. [54], ▷ Lowry et al. [55], ◁ Dirrenberger et al. [56], △ Bosschaart et al. [57], ▽ Kishore et al. [58], ⬡ Hassan et al. [51], ☆ Jomaas et al. [59], ✜ Vagelopoulos et al. [60], ◇ Dyakov et al. [61], ⊠ Park et al. [48], ⬠ Aung et al. [62]

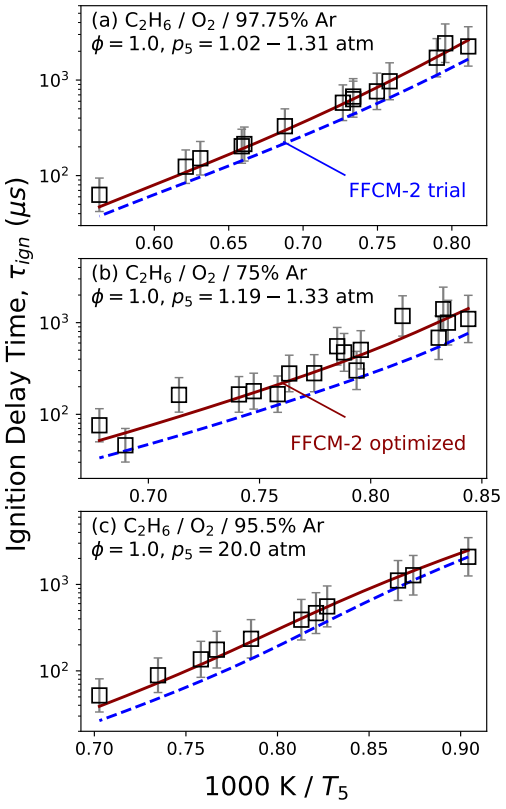

Fig. 9: Experimental (symbols) and computed (lines) ignition delay times for the stoichiometric C_2H_6-O_2 mixtures diluted in Ar. Trial model: dash lines, the optimized FFCM-2: solid lines. Panel (a): C_2H_6-O_2-97.75% Ar, p_5 = 1.02 – 1.31 atm from Devries et al. [63]; panel (b): C_2H_6-O_2-75% Ar, p_5 = 1.19 – 1.33 atm from Aul et al. [34]; panel (c): C_2H_6-O_2-95.5% Ar, p_5 = 20 atm from Hu et al. [47]. Vertical bars are 2σ data uncertainties.

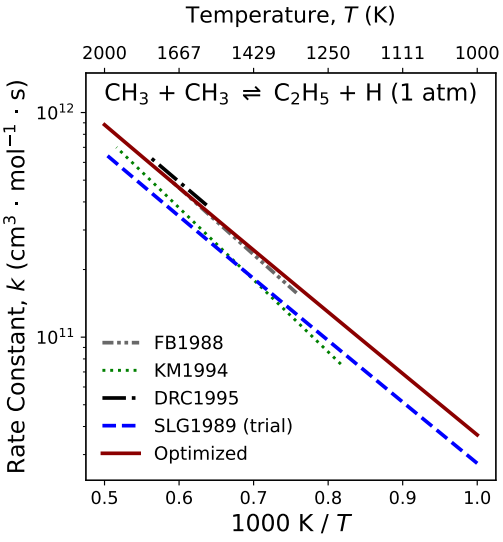

Fig. 10: Arrhenius plot for reaction $CH_3 + CH_3 \rightleftharpoons C_2H_5 + H$. Trial model: dashed line, the optimized FFCM-2: solid line. The trial value was a fit to RRKM calculations by Stewart et al. [64] (SLG1989). The dotted line, dashed dot line, and dash dot dotted line are shock tube measurements by Kim and Michael [65] (KM1994), Davidson et al. [66] (DRC1995) and Frank and Braun-Unkhoff [67] (FB1988), respectively.

3.4.5. Methyl radical recombination

Methyl radicals recombine and dissociate into the ethyl and H radicals via a chemically activated reaction (Reaction (9)),

$$CH_3 + CH_3 \rightleftharpoons C_2H_5 + H. \quad (9)$$

In ethane combustion, Reaction (9) acts in the reverse direction and can be inhibited if CH_3 is present. The consumption of ethyl radical by Reaction (9) also competes with the ethyl decomposition Reaction (8) to produce C_2H_4 and H radical. Figure 11 compares the sensitivity coefficients for ignition delay time under low (p_5 = 0.5 atm) to high (p_5 = 20 atm) pressures. The results show that sensitivity to Reaction (9) decreases with increasing pressure, as Reaction (8) is favored at higher pressures.

In this work, the rate constant of Reaction (9) in the trial model was derived from a pressure dependent fit to the RRKM calculations by Stewart et al. [64]. In the optimized model, the rate coefficient from the data assimilation was increased by a factor of 1.34 from the trial value, with x = 0.421. The uncertainty factor was reduced from f_{trial} = 2.0 to f_{opt} = 1.63. Note that in [6] the same source reaction rate was used as the trial value in the optimization of GRI-Mech 3.0 and was subsequently increased by a factor of 1.37, consistent with the adjusted rate found in our work.

Reaction (9) has been examined using shock tubes by various researchers. Figure 10 compares the trial and optimized rate coefficients found in literature. Davidson et al. [66] measured the species time-history of the CH_3 radical to study the rate coefficients of a series of methyl-methyl reactions, which included Reaction (9). The rate coefficient was determined in the temperature range T = 1570 – 1780 K. This rate is consistent with Frank and Braun-Unkhoff [67], who used the H-atom resonance absorption spectroscopy (ARAS) approach. Kim and Michael determined the rate coefficients in the temperature range T = 1224 – 1938 K [65]. Their rate coefficient was 15-25% lower than that of Frank and Braun-Unkhoff [67] in the region where their temperature regions overlapped. In this work, the optimized rate parameter is consistent with the value reported by Davidson et al. [66].

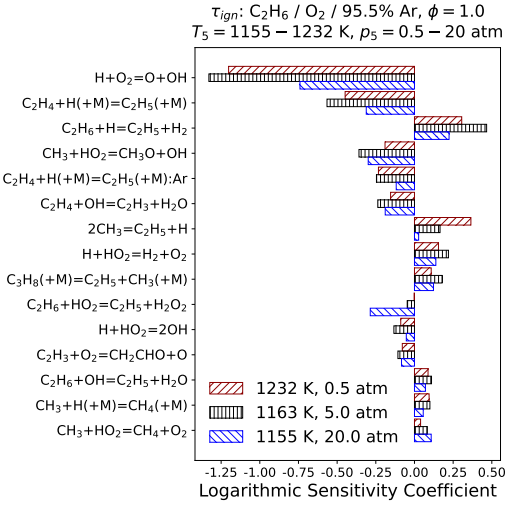

Fig. 11: Ranked sensitivity coefficients for ignition delay times of the stoichiometric C_2H_6/O_2 mixture diluted in 95.5% Ar under selected thermodynamic conditions: T_5 = 1232 K, p_5 = 20.0 atm. (forward slash); T_5 = 1163 K, p_5 = 5.0 atm (vertical) and T_5 = 1155 K, p_5 = 0.5 atm (backslash)

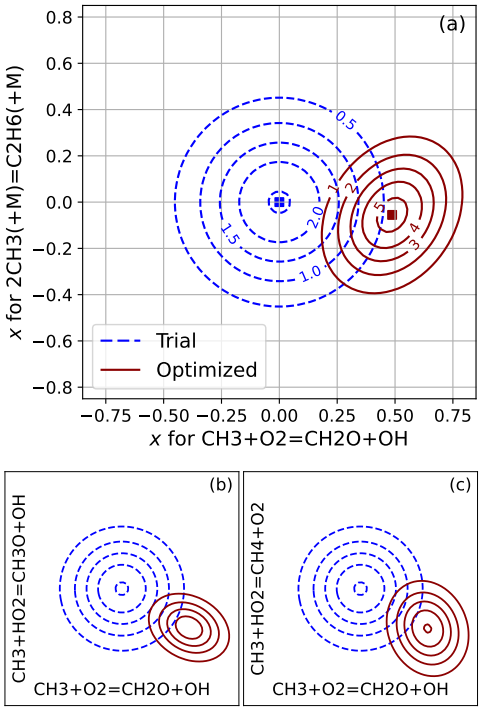

Fig. 12: Contour plots of PDF of $CH_3 + O_2 \rightleftharpoons CH_2O + OH$ (horizontal axis) with four correlated reactions. Dashed circles correspond to the prior model and solid ellipses represent the posterior model. Values on the circles and ellipses in (a) represent the values of the corresponding PDF.

3.5. Revealing kinetic coupling between rate constants

Similar to the FFCM-1 effort, a unique advantage to FFCM-2 is that the availability of the posterior covariance matrix. The posterior covariance matrix Σ defines a multivariate normal distribution of the model's rate parameters. This enables computation of a joint probability density function (PDF) for any set of rate coefficients, quantifying the kinetic coupling between reactions. In this work, we study the aforementioned $CH_3 + O_2$ system due to its known strong coupling effect. Figure 12 shows the joint PDF of Reaction (4) with the three coupled reactions:

$$2\,CH_3\,(+M) \rightleftharpoons C_2H_6\,(+M), \quad (10)$$

$$CH_3 + HO_2 \rightleftharpoons CH_3O + OH, \quad (11)$$

$$CH_3 + HO_2 \rightleftharpoons CH_4 + O_2, \quad (12)$$

The centered, dashed blue circles represent the trial parameter space, obtained by assuming independent multivariate normal distribution for each pair of reaction [68]. The solid ellipses represent the posterior space where the uncertainly was reduced with respect to the trial parameter space. For clarity, we compare Reaction (4) and Reaction (10) in Fig. 12a using a joint PDF distribution plot with contour labels and grid-lines for the normalized rate constants. This level of detail is omitted in other distribution plots, where only qualitative behavior is required for the analysis.

Reactions (11) and (12) both correlate negatively with Reaction (4) as shown in Fig. 12, i.e., if the rate coefficient of the former reaction increases then those of the latter are more likely to decrease; this is indicated by the negative slope of the major axis for the red ellipses. The rate changes supported this correlation during optimization; the mean rate constants for both reactions were reduced, while the rate of Reaction (4) increased, indicating that their coupling influenced the optimization process.

We also consider the sensitivity to target combustion properties to further analyze the coupling of these reactions. Combustion properties, such as ignition delay time, are sensitive to Reactions (4), (11), and (12) where CH_3 is abundant, this includes systems with hydrocarbons beyondCH_4. For example, CH_3 is a key decomposition product of C_3H_8, n-C_4H_{10} and CH_3COCH_3 and a property like ignition delay times of these fuels can contribute to the changes of the aforementioned three reactions during optimization. A strong signal of decreasing the rate coefficient of Reaction (11), derived from the gradient of the objective function, Eq. (1), was due to the under-prediction of ignition delay times for C_3H_8/O_2 mixtures diluted in 91.2% Ar under temperature T_5 = 1114 K and pressure p_5 = 29.5 atm. The fact that Reaction (4) shows

strong kinetic coupling with other reaction pathways and that it impacts an array of combustion property data indicates why large uncertainty is present in literature. The analyses from this work indicate that certain reactions need to be constrained by a joint effort from kinetic targets of multiple species.

4. Conclusions

We demonstrated that data assimilation with proper physical constraints can yield useful kinetic insights in reaction models, using as examples several kinetic case studies from the FFCM-2 model development. In the high pressure CH_4 ignition analysis, we demonstrated that data assimilation is capable of producing insights to identify missing reactions and refine the rate constants of the newly discovered reaction pathways. In the analyses of high-temperature C_2H_4 ignition, we showed that data assimilation offers insights on the branching ratio. Additionally, we showed for five selected reactions that data assimilation is useful in constraining existing rate constants where literature studies have notable uncertainties. We also demonstrated a case study for the kinetic coupling effect of the CH_3 + O_2 system and highlighted the necessity and unique benefit of using a systematic, constrained optimization approach to improve rate constants. We also considered the sensitivity to target combustion properties to further analyze the coupling of theCH_3 + O_2 system. These sensitivities indicated that certain rate constants could be better constrained by a systematic optimization against targets of all species, rather than using a linear sensitivity-based approach against a small set of experiments.

CrediT authorship contribution statement

- Yue Zhang: Data curation, Formal analysis, Investigation, Methodology, Software, Validation, Visualization, Writing - original draft, Writing - review & editing;
- Wendi Dong: Investigation, Software, Validation, Visualization, Writing - original draft, Writing - review & editing;
- Andrea Nobili: Writing - review & editing;
- Ryan F. Johnson: Writing - review & editing;
- Gregory P. Smith: Data curation, Methodology, Writing - review & editing;
- Hai Wang: Conceptualization, Formal analysis, Funding acquisition, Methodology, Project administration, Resources, Supervision, Validation, Writing - review & editing.

Declaration of competing interest

The authors declare that they have no known competing financial interests or personal relationships that could have appeared to influence the work reported in this paper.

Acknowledgments

We acknowledge support through the Office of Naval Research (ONR) Grant Nos. N00014-21-1-2475 and N00014-23-1-2501 with Dr. Eric Marineau as Program Manager, and Grant No. N00014-22-1-2606 with Dr. Steven Martens as Program Manager.

References

[1] H. Wang, Chapter 14 - uncertainty quantification and minimization, in: T. Faravelli, F. Manenti, E. Ranzi (Eds.), Mathematical Modelling of Gas-Phase Complex Reaction Systems: Pyrolysis and Combustion, Vol. 45 of Computer Aided Chemical Engineering, Elsevier, 2019, pp. 723–762.

[2] H. Wang, D. A. Sheen, Combustion kinetic model uncertainty quantification, propagation and minimization, Prog. Energy Combust. Sci. 47 (2015) 1–31.

[3] Z. Hong, D. Davidson, E. Barbour, R. Hanson, A new shock tube study of the h + o_2 → oh + o reaction rate using tunable diode laser absorption of h_2o near 2.5 μm, Proc. Combust. Inst. 33 (2011) 309–316.

[4] J. A. Miller, R. Sivaramakrishnan, Y. Tao, C. F. Goldsmith, M. P. Burke, A. W. Jasper, N. Hansen, N. J. Labbe, P. Glarborg, J. Zádor, Combustion chemistry in the twenty-first century: Developing theory-informed chemical kinetics models, Progress in Energy and Combustion Science 83 (2021) 100886.

[5] M. Frenklach, H. Wang, M. J. Rabinowitz, Optimization and analysis of large chemical kinetic mechanisms using the solution mapping method—combustion of methane, Prog. Energy Combust. Sci. 18 (1992) 47–73.

[6] G. Smith, GRIMech - An optimized detailed chemical reaction mechanism for methane combustion, available at `http://www.me.berkeley.edu/gri_mech` (1999).

[7] Z. Qin, V. V. Lissianski, H. Yang, W. C. Gardiner, S. G. Davis, H. Wang, Combustion chemistry of propane: A case study of detailed reaction mechanism optimization, Proc. Combust. Inst. 28 (2000) 1663–1669.

[8] S. G. Davis, A. V. Joshi, H. Wang, F. Egolfopoulos, An optimized kinetic model of H2/CO combustion, Proc. Combust. Inst. 30 (2005) 1283–1292.

[9] G. P. Smith, Y. Tao, H. Wang, Foundational Fuel Chemistry Model Version 1.0 (FFCM-1), available at `https://web.stanford.edu/group/haiwanglab/FFCM1/pages/FFCM1.html` (2016).

[10] T. Varga, T. Nagy, C. Olm, I. G. Zsély, R. Pálvölgyi, É. Valkó, G. Vincze, M. Cserháti, H. J. Curran, T. Turányi, Optimization of a hydrogen combustion mechanism using both direct and indirect measurements, Proc. Combust. Inst. 35 (2015) 589–596.

[11] T. Varga, C. Olm, T. Nagy, I. G. Zsély, É. Valkó, R. Pálvölgyi, H. J. Curran, T. Turányi, Development

of a Joint Hydrogen and Syngas Combustion Mechanism Based on an Optimization Approach, International Journal of Chemical Kinetics 48 (8) (2016) 407–422.

[12] C. Olm, T. Varga, É. Valkó, S. Hartl, C. Hasse, T. Turányi, Development of an Ethanol Combustion Mechanism Based on a Hierarchical Optimization Approach, International Journal of Chemical Kinetics 48 (8) (2016) 423–441.

[13] V. Samu, T. Varga, K. Brezinsky, T. Turányi, Investigation of ethane pyrolysis and oxidation at high pressures using global optimization based on shock tube data, Proceedings of the Combustion Institute 36 (1) (2017) 691–698.

[14] C. Olm, T. Varga, É. Valkó, H. J. Curran, T. Turányi, Uncertainty quantification of a newly optimized methanol and formaldehyde combustion mechanism, Combust. Flame 186 (2017) 45–64.

[15] Z. Zhou, K. Lin, Y. Wang, J. Wang, C. K. Law, B. Yang, OptEx: An integrated framework for experimental design and combustion kinetic model optimization, Combustion and Flame 245 (2022) 112298.

[16] Y. Zhang, W. Dong, L. Vandewalle, R. Xu, G. Smith, H. Wang, Foundational Fuel Chemistry Model Version 2.0 (FFCM-2), available at `https://web.stanford.edu/group/haiwanglab/FFCM2/` (2023).

[17] D. A. Sheen, H. Wang, The method of uncertainty quantification and minimization using polynomial chaos expansions, Combust. Flame 158 (2011) 2358–2374.

[18] D. A. Sheen, X. You, H. Wang, T. Løvås, Spectral uncertainty quantification, propagation and optimization of a detailed kinetic model for ethylene combustion, Proc. Combust. Inst. 32 (2009) 535–542.

[19] Y. Zhang, W. Dong, L. A. Vandewalle, R. Xu, G. P. Smith, H. Wang, Neural network approach to response surface development for reaction model optimization and uncertainty minimization, Combust. Flame 251 (2023) 112679.

[20] Y. Zhang, W. Dong, R. Xu, G. P. Smith, H. Wang, Foundational fuel chemistry model 2–iso-butene chemistry and application in modeling alcohol-to-jet fuel combustion, Combustion and Flame 259 (2024) 113168.

[21] W. Dong, Y. Zhang, G. P. Smith, H. Wang, Aspects of fundamental reaction kinetics and legacy combustion properties in data-assimilated combustion reaction model development, Proceedings of the Combustion Institute 40 (1-4) (2024) 105410.

[22] Y. Zhang, Neural network assisted combustion chemistry reaction model optimization and uncertainty minimization, Ph.D. thesis, Stanford University, United States (2023).

[23] S. Lakshmanan, W. L. Hase, G. P. Smith, Mechanism and kinetics for the reaction of methyl peroxy radical with o2, Phys. Chem. Chem. Phys. 23 (2021) 23508–23516.

[24] J. Shao, R. Choudhary, D. F. Davidson, R. K. Hanson, S. Barak, S. Vasu, Ignition delay times of methane and hydrogen highly diluted in carbon dioxide at high pressures up to 300 atm, Proc. Combust. Inst. 37 (2019) 4555–4562.

[25] E. L. Petersen, D. F. Davidson, R. K. Hanson, Ignition Delay Times of Ram Accelerator CH/O/Diluent Mixtures, J. Propul. Power 15 (1999) 82–91.

[26] D. Baulch, C. T. Bowman, C. J. Cobos, R. A. Cox, T. Just, J. Kerr, M. Pilling, D. Stocker, J. Troe, W. Tsang, et al., Evaluated kinetic data for combustion modeling: Supplement II, Journal of physical and chemical reference data 34 (2005) 757–1397.

[27] X. Li, A. W. Jasper, J. Zádor, J. A. Miller, S. J. Klippenstein, Theoretical kinetics of O + C_2H_4, Proc. Combust. Inst. 36 (2017) 219–227.

[28] F. R. Gillespie, An experimental and modelling study of the combustion of oxygenated hydrocarbons, Ph.D. thesis (2014).

[29] D. C. Horning, A study of the high temperature autoignition and thermal decomposition of hydrocarbons, Ph.D. thesis (2001).

[30] C.-L. Yu, C. Wang, M. Frenklach, Chemical Kinetics of Methyl Oxidation by Molecular Oxygen, The Journal of Physical Chemistry 99 (1995) 14377–14387.

[31] R. Zhu, C.-C. Hsu, M. C. Lin, Ab initio study of the CH_3+O_2 reaction: Kinetics, mechanism and product branching probabilities, J. Chem. Phys. 115 (2001) 195–203.

[32] N. K. Srinivasan, M.-C. Su, J. W. Sutherland, J. V. Michael, Reflected Shock Tube Studies of High-Temperature Rate Constants for CH_3 + O_2, H_2CO + O_2, and OH + O_2, J. Phys. Chem. A 109 (2005) 7902–7914.

[33] J. T. Herbon, R. K. Hanson, C. T. Bowman, D. M. Golden, The reaction of ch_3+ o_2: experimental determination of the rate coefficients for the product channels at high temperatures, Proc. Combust. Inst. 30 (2005) 955–963.

[34] C. J. Aul, W. K. Metcalfe, S. M. Burke, H. J. Curran, E. L. Petersen, Ignition and kinetic modeling of methane and ethane fuel blends with oxygen: A design of experiments approach, Combust. Flame 160 (2013) 1153–1167.

[35] F. Zhang, C. Huang, B. Xie, X. Wu, Revisiting the chemical kinetics of CH_3 + O_2 and its impact on methane ignition, Combust. Flame 200 (2019) 125–134.

[36] I. Alecu, D. G. Truhlar, Computational study of the reactions of methanol with the hydroperoxyl and methyl radicals. 2. Accurate thermal rate constants, J. Phys. Chem. A 115 (2011) 14599–14611.

[37] S. J. Klippenstein, L. B. Harding, M. J. Davis, A. S. Tomlin, R. T. Skodje, Uncertainty driven theoretical kinetics studies for CH_3OH ignition: HO_2+CH_3OH and O_2+CH_3OH, Proc. Combust. Inst. 33 (2011) 351–357.

[38] M. Altarawneh, A. H. Al-Muhtaseb, B. Z. Dlugogorski, E. M. Kennedy, J. C. Mackie, Rate constants for hydrogen abstraction reactions by the hydroperoxyl radical from methanol, ethenol, acetaldehyde, toluene, and phenol, J. Comput. Chem. 32 (2011) 1725–1733.

[39] J. A. Manion, D. A. Sheen, I. A. Awan, Evaluated Kinetics of the Reactions of H and CH3 with n-Alkanes: Experiments with n-Butane and a Combustion Model Reaction Network Analysis, J. Phys. Chem. A 119 (2015) 7637–7658.

[40] N. Cohen, The use of transition-state theory to extrapolate rate coefficients for reactions of h atoms with alkanes, International journal of chemical kinetics 23 (1991) 683–700.

[41] H.-H. Carstensen, A. M. Dean, Rate Constant Rules for the Automated Generation of Gas-Phase Reaction Mechanisms, J. Phys. Chem. A 113 (2009) 367–380.

[42] S. L. Peukert, R. Sivaramakrishnan, J. V. Michael, High temperature rate constants for H/D+n-C_4H_{10} and i-C_4H_{10}, Proc. Combust. Inst. 35 (2015) 171–179.

[43] R. R. Baker, R. R. Baldwin, R. W. Walker, Addition of n-butane to slowly reacting mixtures of hydrogen and oxygen at 480° c. part 2.—formation of oxygenated products, Journal of the Chemical Society, Faraday Transactions 1: Physical Chemistry in Condensed Phases 71 (1975) 756–779.

[44] J. A. Miller, S. J. Klippenstein, The H + C2H2 (+M) = C2H3 (+M) and H + C2H2 (+M) = C2H5 (+M) reactions: Electronic structure, variational transition-state theory, and solutions to a two-dimensional master equation, Phys. Chem. Chem. Phys. 6 (2004) 1192–1202.

[45] J. Zhang, E. Hu, Z. Zhang, L. Pan, Z. Huang, Comparative Study on Ignition Delay Times of C1–C4 Alkanes, Energy Fuels 27 (2013) 3480–3487.

[46] L. Pan, Y. Zhang, J. Zhang, Z. Tian, Z. Huang, Shock tube and kinetic study of C2H6/H2/O2/Ar mixtures at elevated pressures, Int. J. Hydrogen Energy 39 (2014) 6024–6033.

[47] E. Hu, Y. Chen, Z. Zhang, X. Li, Y. Cheng, Z. Huang, Experimental Study on Ethane Ignition Delay Times and Evaluation of Chemical Kinetic Models, Energy Fuels 29 (2015) 4557–4566.

[48] O. Park, P. S. Veloo, F. N. Egolfopoulos, Flame studies of C_2 hydrocarbons, Proc. Combust. Inst. 34 (2013) 711–718.

[49] H. Hashemi, J. G. Jacobsen, C. T. Rasmussen, J. M. Christensen, P. Glarborg, S. Gersen, M. van Essen, H. B. Levinsky, S. J. Klippenstein, High-pressure oxidation of ethane, Combust. Flame 182 (2017) 150–166.

[50] W. K. Metcalfe, S. M. Burke, S. S. Ahmed, H. J. Curran, A Hierarchical and Comparative Kinetic Modeling Study of C1 − C2 Hydrocarbon and Oxygenated Fuels, Int. J. Chem. Kinet. 45 (2013) 638–675.

[51] M. I. Hassan, K. T. Aung, O. C. Kwon, G. M. Faeth, Properties of laminar premixed hydrocarbon/air flames at various pressures, J. Propul. Power 14 (1998) 479–488.

[52] F. N. Egolfopoulos, D. L. Zhu, C. K. Law, Experimental and numerical determination of laminar flame speeds: Mixtures of C_2-hydrocarbons with oxygen and nitrogen, Symposium (International) on Combustion 23 (1990) 471–478.

[53] M. Goswami, R. J. Bastiaans, L. P. De Goey, A. A. Konnov, Experimental and modelling study of the effect of elevated pressure on ethane and propane flames, Fuel 166 (2016) 410–418.

[54] S. Ravi, T. G. Sikes, A. Morones, C. L. Keesee, E. L. Petersen, Comparative study on the laminar flame speed enhancement of methane with ethane and ethylene addition, Proc. Combust. Inst. 35 (2015) 679–686.

[55] W. Lowry, J. De Vries, M. Krejci, E. Petersen, Z. Serinyel, W. Metcalfe, H. Curran, G. Bourque, Laminar flame speed measurements and modeling of pure alkanes and alkane blends at elevated pressures, J. Eng. Gas Turbines Power 133 (Sep. 2011).

[56] P. Dirrenberger, P. A. Glaude, R. Bounaceur, H. Le Gall, A. P. Da Cruz, A. A. Konnov, F. Battin-Leclerc, Laminar burning velocity of gasolines with addition of ethanol, Fuel 115 (2014) 162–169.

[57] K. J. Bosschaart, L. P. De Goey, The laminar burning velocity of flames propagating in mixtures of hydrocarbons and air measured with the heat flux method, Combust. Flame 136 (2004) 261–269.

[58] V. R. Kishore, N. Duhan, M. R. Ravi, A. Ray, Measurement of adiabatic burning velocity in natural gas-like mixtures, Exp. Therm. Fluid Sci. 33 (2008) 10–16.

[59] G. Jomaas, X. L. Zheng, D. L. Zhu, C. K. Law, Experimental determination of counterflow ignition temperatures and laminar flame speeds of C_2–C_3 hydrocarbons at atmospheric and elevated pressures, Proc. Combust. Inst. 30 (2005) 193–200.

[60] C. M. Vagelopoulos, F. N. Egolfopoulos, Direct experimental determination of laminar flame speeds, Symposium (International) on Combustion 27 (1998) 513–519.

[61] I. V. Dyakov, J. De Ruyck, A. A. Konnov, Probe sampling measurements and modeling of nitric oxide formation in ethane + air flames, Fuel 86 (2007) 98–105, publisher: Elsevier.

[62] K. T. Aung, L. K. Tseng, M. A. Ismail, G. M. Faeth, Response to comment by S.C. Taylor and D.B. Smith on "Laminar burning velocities and Markstein numbers of hydrocarbon/air flames", Combust. Flame 102 (1995) 526–530, publisher: Elsevier.

[63] J. Devries, J. Hall, S. Simmons, M. Rickard, D. Kalitan, E. Petersen, Ethane ignition and oxidation behind reflected shock waves, Combust. Flame 150 (2007) 137–150.

[64] P. Stewart, C. Larson, D. Golden, Pressure and temperature dependence of reactions proceeding via a bound complex. 2. Application to $2CH_3 \rightarrow C_2H_5 + H$, Combust. Flame 75 (1989) 25–31.

[65] K. P. Kim, J. V. Michael, The thermal reactions of CH_3, Symposium (International) on Combustion 25 (1994) 713–719.

[66] D. F. Davidson, M. D. D. Rosa, E. J. Chang, R. K. Hanson, C. T. Bowman, A shock tube study of methyl-methyl reactions between 1200 and 2400 K, Int. J. Chem. Kinet. 27 (1995) 1179–1196.

[67] P. Frank, M. Braun-Unkhoff, Shock tubes and waves, Proceedings of the 16th International Symposium on Shock Tubes and Waves (Jul. 1988).

[68] D. A. Sheen, H. Wang, Combustion kinetic modeling using multispecies time histories in shock-tube oxidation of heptane, Combust. Flame 158 (2011) 645–656.